

Dielectric properties of polyamide 12-chromium (III) oxide nanocompositesE. S. Shapoval¹, V. V. Zuev^{1,2}¹ITMO University, Kronverkskiy pr., 49, 197101 St. Petersburg, Russia²Institute of Macromolecular Compounds of the Russian Academy of Sciences,
Bolshoi pr., 31, 199004 St. Petersburg, Russia

katenka-shapoval@yandex.ru; zuev@hq.macro.ru

PACS 81.07.Lb**DOI 10.17586/2220-8054-2016-7-3-472-478**

Broadband dielectric spectroscopy was employed to study polymer nanocomposites based on PA12 filled with different loading (0.1 – 10 wt.%) of nanosized (average grain size of about 1 – 5 nm) chromium (III) oxide. The experimental dielectric data were analyzed within the formalisms of complex permittivity and electric modulus. Three relaxation processes and Maxwell–Wagner–Sillars (MWS) interfacial polarizations were observed. It was found that all the relaxations were sensitive to filler contents. The presence of nanosized amphoteric chromium (III) oxide was shown to lead to the softening of the polyamide matrix that manifested in decrease of the activation energy of the α - and β -relaxation processes and glass transition temperatures. The softening of polymer matrix is the reason for the decrease in the mechanical properties of the polymer nanocomposites as compared to that of neat PA12.

Keywords: nanocomposites, polyamide 12, chromium (III) oxide, relaxation processes, activation energy dielectric spectroscopy.

Received: 8 February 2016

Revised: 19 March 2016

1. Introduction

Polymer magnetic materials can potentially find a great number of applications in different fields such as data storage, biomedicine, biosensors, drug delivery agent, magnetic resonance imaging devices, and a range of others [1–4]. Theoretical modeling predicts that the mechanical properties of polymer nanocomposites should be superior to those of conventional composites [5,6]. These improved properties are attained at lower filler content in comparison to conventionally filled polymers. However, the introduction of nanosized particles of magnetic oxides into different polymer matrices leads to a decrease in the mechanical properties. This was shown for the introduction of nanosized oxide F_3O_4 into polyurethane [7]. We obtained similar results for the preparation of polymer nanocomposites based on PA12 filled with different loading (0.1 – 10 wt.%) of nanosized (average grain size of about 1 – 5 nm) chromium (III) oxide [8]. It was suggested that the introduction of new fracture mechanisms, rigidity augmentation, and pronounced filler-filler interactions were responsible for the observed behavior instead of filler-polymer interactions [9–12]. The dynamics of polymer matrix changes due to changes in interactions with nanosized filler particles. The polymer dynamics and the glass transition in polymer nanocomposites are more complex than in neat polymer [13]. Here, we use broadband dielectric spectroscopy (BDS) to directly measure the influence of nanoparticles on polymer relaxations corresponding to different lengths and time scales. BDS is one of the most efficient tools for studying the molecular relaxations of polymers. It covers a broad frequency range, allowing measurement of different relaxation processes simultaneously, and even entire chain relaxation processes under favorable circumstances [14]. Relaxation processes in a polymer matrix are clearly connected with its mechanical properties. The β -relaxation is phenomenologically linked to the mechanical properties of polymeric materials [15, 16]. The α -relaxation is connected with the onset of large-scale motions of the chain segments in the vicinity of T_g and determined viscoelastic behavior. The aim of the present work is to provide a description of the relaxation processes for PA12/Cr₂O₃ nanocomposites over a range of temperatures and frequencies. As with any thermoplastic nanocomposites, a description of the relaxation processes parameters is of great interest, and is central for rational approach to thermomechanical processing.

2. Experimental

PA12/Cr₂O₃ nanocomposites were synthesized according [8]. Dielectric measurements were performed using an Alpha Analyzer combined with a Quatro Temperature Control system unit that provides temperature stability of 0.1 °C, both by Novocontrol. Complex dielectric permittivity $\varepsilon^*(f) = \varepsilon'(f) - i\varepsilon''(f)$ was measured isothermally in steps of 5 °C from –150 to +200 °C and over frequencies ranging from 10^{-2} to 10^6 Hz. The nanocomposite

films were placed and melted in a parallel-plate copper capacitor with 20 mm diameter, and a pair of glass fiber with 80 μm diameter was used as the spacers between electrodes.

3. Results and discussion

Plots of the three-dimensional real and imaginary parts, ϵ' and ϵ'' , of the complex dielectric permittivity ϵ^* versus frequency and temperature are presented in Fig. 1 for the sample with 5 wt.% of Cr_2O_3 .

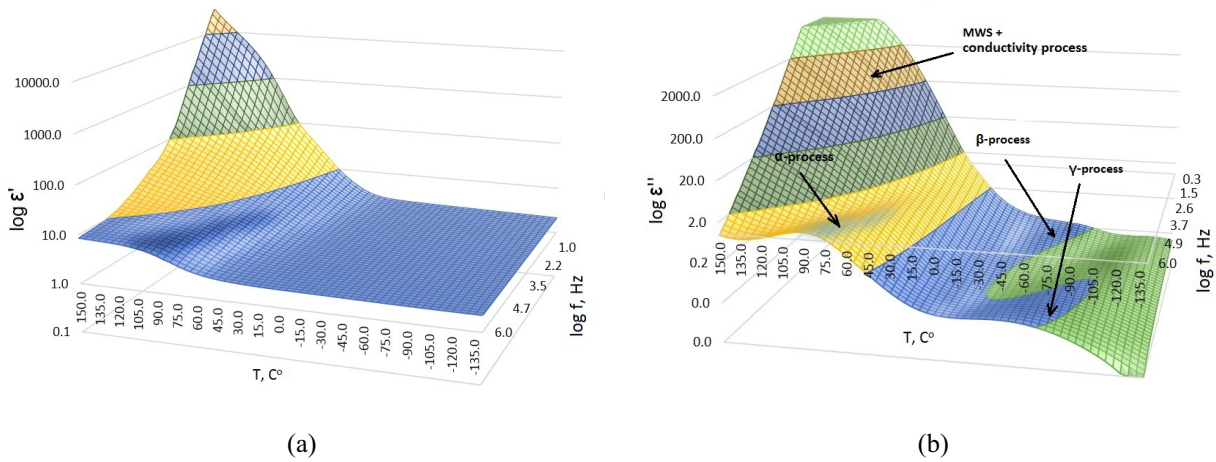


FIG. 1. 3D plot of ϵ' (a) and ϵ'' (b) versus frequency and temperature for nanocomposite with 5 wt.% of nanosized Cr_2O_3

The main relaxation processes identified are the same as those found for pure PA12 [17]: (1) the γ -relaxation appeared between 170 K and 250 K; (2) the β -relaxation appeared between 230 K and 275 K; (3) the segmental α -relaxation occurred between 270 K and 350 K; (4) the MWS/conductivity process visible in the high temperature regime arising from the drift motion of the charges and charge carriers blocked at the interphase between amorphous and crystalline regions and conductivity effects. The four processes are typically for PAs [18] and were observed in all studied samples.

The isochronal graph at 1 kHz, Fig. 2, shows the temperature dependence of ϵ' and ϵ'' for neat PA12 and composites. The differences between samples are noted, especially at higher temperatures, where the MWS/conductivity process is located.

It should be noted that in the ϵ'' (f) plots (Fig. 2b) only an α loss peak was observed. MWS relaxation can be masked by large conduction effects at high temperatures. Moreover, the peak is superimposed by electrode

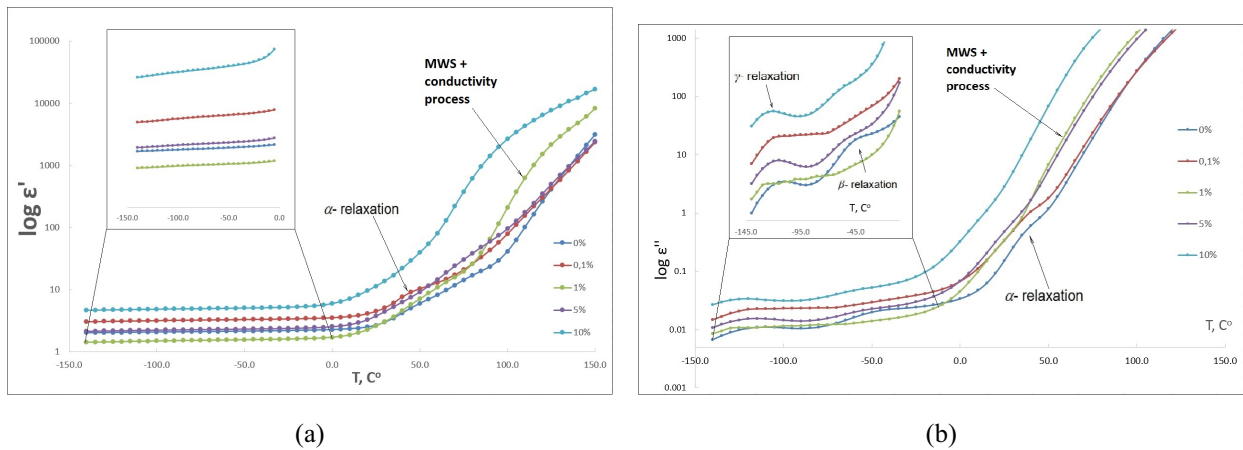


FIG. 2. Temperature dependence of ϵ' (a) and ϵ'' (b) for neat PA12 and all nanocomposites at a frequency of 1 kHz

polarization effects, and therefore not be clearly extracted in the permittivity spectra. Using the complex electric modulus formalism the MWS/conductivity process is visible as a peak in the imaginary part M'' of the complex dielectric modulus M^* . M^* is related to ε^* as follows [19]:

$$M^* = \frac{1}{\varepsilon^*} = M' + iM'',$$

$$M' = \frac{\varepsilon'}{\varepsilon'^2 + \varepsilon''^2} \quad \text{and} \quad M'' = \frac{\varepsilon''}{\varepsilon'^2 + \varepsilon''^2}.$$

A plot of M'' versus frequency and temperature for the sample with 5 wt.% of Cr_2O_3 is shown in Fig. 3.

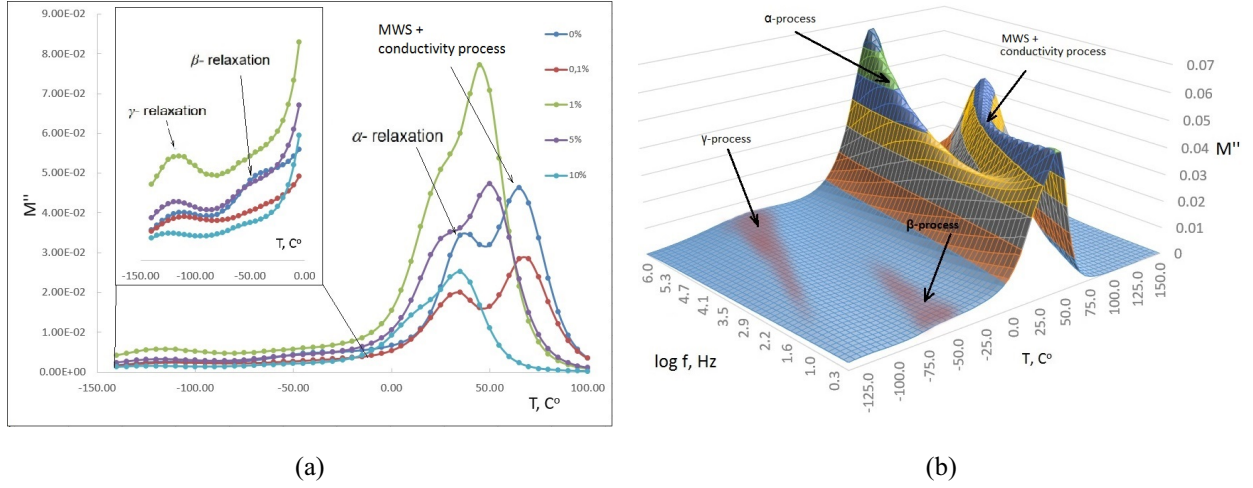


FIG. 3. (a) 3D plot of M'' versus frequency and temperature for nanocomposite with 5 wt.% of nanosized Cr_2O_3 and (b) temperature dependence of M'' for neat PA12 and all nanocomposites at a frequency of 1 kHz

The MWS/conductivity process can now be identified as a peak in the higher frequency regime. In order to evaluate the individual relaxation processes quantitatively, a model function has been fitted to the dielectric data, with the Havriliak-Negami (H-N) phenomenological relation [20]:

$$\varepsilon^*(\omega) = \varepsilon_\infty + \frac{\Delta\varepsilon}{\left(1 + (i\omega\tau_{NH})^{1-\alpha}\right)^\beta}, \quad (1)$$

in its most general form. In this expression, $\varepsilon^* = \varepsilon' - i\varepsilon''$, is the complex dielectric function, $\omega = 2\pi f$, f is the field frequency, $\Delta\varepsilon$ is the intensity of the dielectric process, $\tau_{NH} = 1/2\pi f_{NH}$ and f_{NH} is the position of the relaxation process on the frequency scale, ε_∞ is $\varepsilon'(f)$ for $f \gg f_{NH}$, α and β are shape parameters representing the symmetrical and asymmetrical broadening of the relaxation with respect to the Debye peak. The main characteristic of each relaxation process is the most probable relaxation time, τ_{\max} , determined according to [21] as

$$\tau_{\max} = \tau_{HN} \left(\frac{\sin\left(\frac{\pi\alpha\beta}{2(\beta+1)}\right)}{\sin\left(\frac{\pi\alpha}{2(\beta+1)}\right)} \right)^{1/\alpha}. \quad (2)$$

Figure 4 shows examples of such fits to the composites' relaxation processes at given temperatures for each process in the measured frequency window.

The α -relaxation is associated with the onset of large-scale motions of the chain segments in the vicinity of T_g . At higher temperatures, near the α -relaxation process, heating is accompanied by the creation of carriers due to the ionization of impurities and breaking of chemical bonds (the N-H bonds, etc). Hence, it is necessary to add an additional term related to the conductivity in Eq. (1):

$$\varepsilon^*(\omega) = \varepsilon_\infty + \frac{\Delta\varepsilon}{\left(1 + (i\omega\tau_{NH})^{1-\alpha}\right)^\beta} - i \left(\frac{\sigma_0}{\omega\varepsilon_0} \right). \quad (3)$$

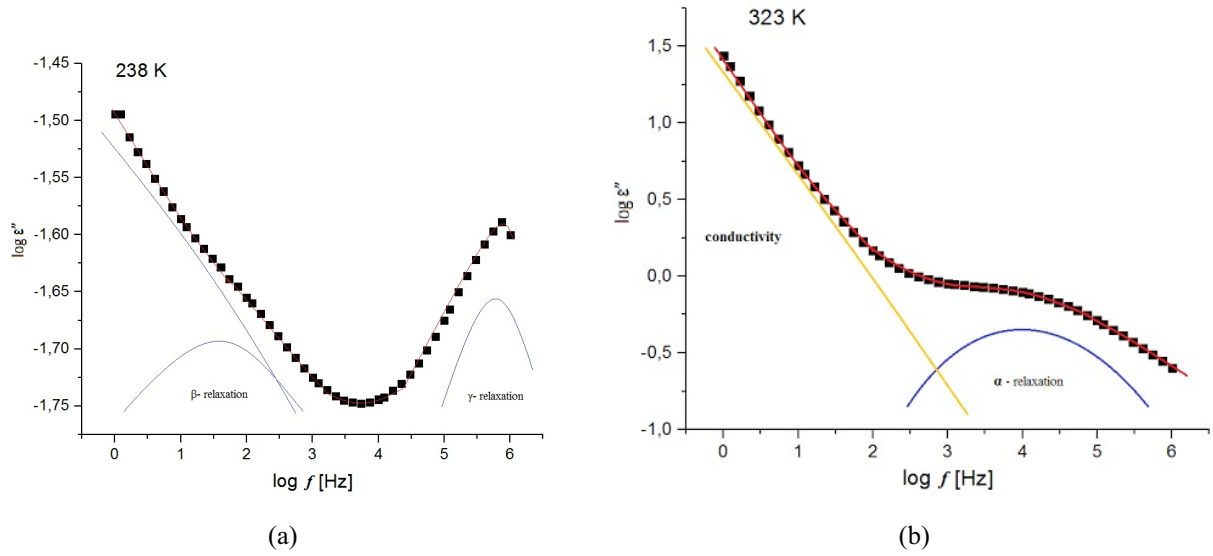


FIG. 4. Isothermal scans (ϵ'' vs frequency) at different fixed temperatures for nanocomposite with 5 wt.% of nanosized Cr_2O_3 . Characteristic temperatures for each process are chosen at which the process is visible in the measured frequency window. (a) γ - and β - relaxation, and (b) α -relaxation. Symbols are the experimental data and full lines represent the total fit

In this equation, σ_0 is the dc conductivity and ϵ_0 is the permittivity of free space (8.854 pF/m). The fitting procedure is complicated very often because of the presence of incomplete peaks, in spite of the frequency window extending over more than 8 orders of magnitude. The quality of the fit is quite good and the characteristic relaxation time for each relaxation process can be extracted. The γ - and β -relaxations are due to relatively shorter chain motions. The dependences of $-\log \tau_{\max}$ on the inverse temperature are linear for all nanocomposites and neat PA12 in the regions of γ and β processes (Fig. 5). As a result, the temperature dependence of these relaxations can be modeled by an Arrhenius type expression (4) [22]:

$$\tau(T)_{\max} = \tau_0 \exp\left(\frac{E_a}{RT}\right). \tag{4}$$

Here, $\tau_0 = \tau_{\max}$ at $T \rightarrow \infty$, E_a is the activation energy. Values of τ_0 and E_a are given in Table 1.

The β -relaxation is phenomenologically linked to the mechanical properties of polymeric materials [15, 16]. From Table 1, one can see that for the composites, both the E_a and Young's modulus decrease. Assignment of molecular motions associated with the β -relaxation is complicated and a number of varying opinions exist in the literature [18, 19]. However, these motions should be associated with the motion of amide groups together with

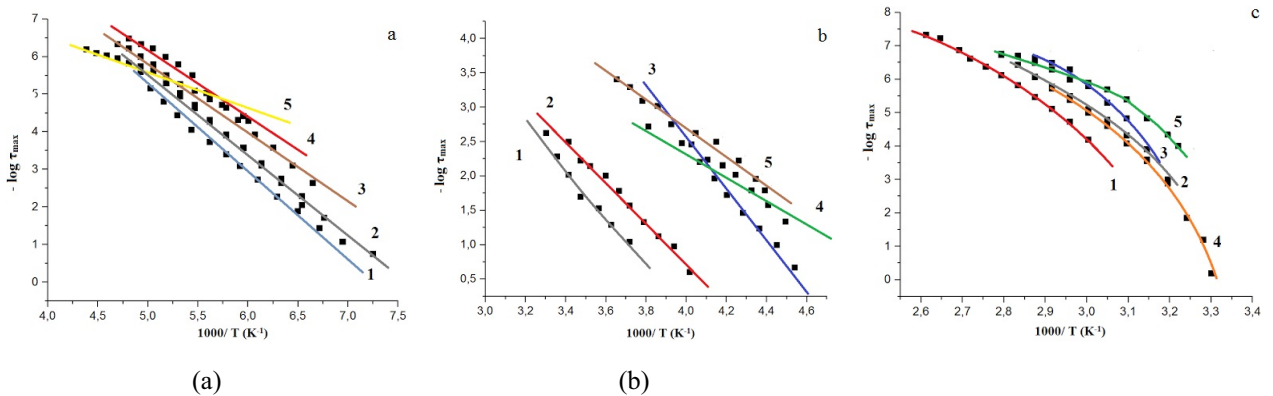


FIG. 5. Dependences of $-\log \tau_{\max}$ on the reciprocal of temperature for neat PA12 (1) and nanocomposites with 0.1 wt.% (2); with 1 wt.% (3); with 5 wt.% (4); and with 10 wt.% (5); (c) α -relaxation; (b) β -relaxation; (a) γ -relaxation

TABLE 1. T_g and parameters of γ , β and α (from VFT fit) relaxation processes of neat PA12 and nanocomposites, where τ_0 is the relaxation time at infinite high temperature, T_0 is so-called Vogel temperature at which the relaxation time goes to infinity, and D is the parameter related to the *fragility* of material

Samples, wt. % Cr ₂ O ₃		E_a , kJ/mol	τ_0 , s	D	T_0 , K	T_g , K	Young's modulus, GPa [8]
0	γ -mode	83.7	3.9×10^{-16}				
	β -mode	59.2	4.4×10^{-13}				
	α -mode	292.4	1.4×10^{-7}	3.32	280	332	0.97
0.1	γ -mode	62.7	3.9×10^{-16}				
	β -mode	48.3	3.9×10^{-13}				
	α -mode	266.6	4.0×10^{-10}	4.25	253	329	0.66
1	γ -mode	80.0	3.1×10^{-16}				
	β -mode	60.25	3.6×10^{-13}				
	α -mode	270.2	1.0×10^{-10}	2.95	267	318	0.49
5	γ -mode	71.4	4.3×10^{-16}				
	β -mode	59.4	2.3×10^{-13}				
	α -mode	279.0	2.3×10^{-10}	3.10	265	315	0.47
10	γ -mode	67.0	3.8×10^{-16}				
	β -mode	52.6	4.9×10^{-13}				
	α -mode	225.0	2.0×10^{-9}	2.47	256	303	0.36

neighboring methylene groups. Cr₂O₃ is an amphoteric oxide which can undergo bonding with the amide group, therefore disrupting the H-bonding network between adjacent polymer chains. This leads to decrease in the E_a of the β -relaxation and, hence, lowering in the Young's modulus. The decrease in the activation energy of the β -relaxation process indicates that the mobility of polymer matrix is a pre-condition for this mechanism to be effective.

The low temperature γ -relaxation involves the motion of short sequences of CH₂ groups connected with an amide group which provides the dielectric activity. As a result, the dependence of E_a of the γ -relaxation on the amount of nanofillers is quite.

The α -relaxation is associated with onset of large-scale motions of the chain segments in the vicinity of T_g . The temperature dependence of the characteristic relaxation times can then be described using the Vogel-Fulcher-Tammann equation [22]:

$$\tau = \tau_0 \exp\left(\frac{DT_0}{T - T_0}\right), \quad (5)$$

where τ_0 is the relaxation time at infinite high temperature, T_0 is so-called Vogel temperature at which the relaxation time goes to infinity, and D is the parameter related to the *fragility* of material [23]. A smaller D value implies a steeper temperature dependence for the relaxation time or a more "fragile" behavior. The D data are given in Table 1. According to Plazek et al. [24, 25] the activation energy of α -relaxation process can be calculated using the following expression:

$$\frac{E_a}{R} = \frac{DT_0}{\left(1 - \frac{T_0}{T_g}\right)^2}, \quad (6)$$

where E_a is the activation energy, R is the gas constant and T_g the glass transition temperature. The values of D and T_0 parameters were extracted from the best fit to equation (3). The values of activation energies for α -relaxation as well as the VFT parameters T_0 , D and T_g are gathered in Table 1. As can see, T_g values of for

the composites decrease in comparison to neat PA12, so the decrease in the moduli upon the introduction of the nanoparticles can be due to a plasticizing effect that the Cr_2O_3 nanoparticles could have exerted on the polymer matrix. However, T_g of the composite with 0.1 wt.% of Cr_2O_3 is very similar (if not identical) to the T_g of the pure polymer, but their Young's modulus is similar to moduli for other composites and is much smaller than that of pure PA12 [8], so the decrease in the moduli upon the introduction of the nanoparticles are not only due to a plasticizing effect. The softening of polymer matrix associated with local mobility (β -relaxation) is probably more important. This effect is opposite to the typical result of nanofiller addition, and is manifested as the well-documented "antiplasticizing phenomenon" [26]. Because of their small size, nanofillers have a high surface-to-volume ratio and provide high-energy surfaces. A desired consequence of embedding nanosized fillers into a polymer matrix is the enhanced bonding between the matrix and additives. The composite theory predicts that improved bonding between polymer matrix and reinforcing phase leads to hindering of polymer chain motions [27]. Despite these predictions, however, BDS investigations of nanocomposites have provided mixed results [28]. We believe that this is caused by the presence of specific intermolecular interactions (e.g., H-bonding), within polymer matrix like PAs which can be influenced by nanoparticles. The nature of these interactions can depend upon both the polymer's and nanoparticles' chemical properties.

At temperatures above α -relaxation, a MWS polarization [29] (Fig. 4) is observed. Moreover, at these temperatures, conductivity effects also play a role, and therefore, both the MWS process and conductivity phenomenon contribute to the high temperature dielectric response. To separate these processes is impossible, therefore they are not considered for further discussion.

4. Conclusions

In the present work, the molecular dynamics of nanocomposites based on PA12 filled with different loadings (0.1 – 10 wt.%) of nanosized (average grain size of about 1 – 5 nm) chromium (III) oxide was investigated by means of dielectric spectroscopy. For all polymer nanocomposites samples, two local relaxation modes, the γ - and β -relaxation, and a segmental α -relaxation was observed. These relaxation modes were evaluated for further analysis. In addition, a high temperature response due to a MWS process combined with conductivity effects was noted.

The E_a of the β -relaxation was shown to decrease for nanocomposites in comparison to neat PA12. The β -relaxation is phenomenologically linked to the mechanical properties of polymeric materials, hence, this observation can explain the Young's modulus decreases for these composites after nanofiller loading. The molecular reason for polymer matrix softening could be related to the disruption of amide H-bonds between neighboring polymer chains after complexation with nanosized chromium (III) oxide. The softening of the polymer matrix associated with local mobility (β -relaxation) is supported by decreases in the glass transition temperatures related to the α -relaxation for all nanocomposites. The E_a of the α -relaxation also decreases, therefore, a plasticizing effect was observed upon the introduction of nanosized chromium (III) oxide into the polyamide matrix.

References

- [1] Yan F., Li J., et al. Preparation of Fe_3O_4 /polystyrene composite particles from monolayer oleic acid modified Fe_3O_4 nanoparticles via miniemulsion polymerization. *J. Nanopart. Res.*, 2009, **11**, P. 289–296.
- [2] Balakrishnan S., Bonder M.J., Hadjipanayis G.C. Particle size effect on phase and magnetic properties of polymer-coated magnetic nanoparticles. *J. Magn. Mater.*, 2009, **321**, P. 117–122.
- [3] Giri S.K., Pradhan G.C., Das N. Thermal, electrical and tensile properties of synthesized magnetite/polyurethane nanocomposites using magnetite nanoparticles derived from waste iron ore tailing. *J. Polym. Res.*, 2014, **21**, 446.
- [4] Kalia S., Kango S., et al. Magnetic polymer nanocomposites for environmental and biomedical applications. *Colloid. Polym. Sci.*, 2014, **292**, P. 2025–2052.
- [5] Vollenberg P.H.T., Heikens D. Particle size dependence of the Young's modulus of filled polymers: 1. Preliminary experiments. *Polymer*, 1989, **30**, P. 1656–1662.
- [6] Gersappe D. Molecular Mechanisms of Failure in Polymer Nanocomposites. *Phys. Rev. Lett.*, 2002, **89**, 058301(1–4).
- [7] Dos Santos L.R., Ligabue R., et al. New magnetic nanocomposites: Polyurethane/ Fe_3O_4 -synthetic talc. *Eur. Polym. J.*, 2015, **69**, P. 38–49.
- [8] Shapoval E.S., Zuev V.V. Novel polyamide 12/ chromium (III) oxide nanoparticles composites: melting behaviour and complex isothermal crystallization kinetics. *Polymer Composites*, 2015, **36** (6), P. 999–1005.
- [9] Jordan J., Jacob K.I., et al. Experimental trends in polymer nanocomposites? a review. *Mater. Sci. Eng. A*, 2005, **393**, P. 1–11.
- [10] Zhu L., Narh K.A. Numerical simulation of the tensile modulus of nanoclay-filled polymer Composites. *J. Polym. Sci. Part B. Polym. Phys.*, 2004, **42**, P. 2391–2406.
- [11] Ciprari D., Jakob K., Tannenbaum R. Characterization of polymer nanocomposites interphase and its impact on the mechanical properties. *Macromolecules*, 2006, **39**, P. 6565–6573.
- [12] Kango S., Kalia S., et al. Surface modification of inorganic nanoparticles for development of organic/inorganic nanocomposites? A review. *Prog. Polym. Sci.*, 2013, **38**, P. 1232–1261.

- [13] Allegra G., Raos G., Vacatello M. Theories and simulations of polymer based nanocomposites: from chain statistics to reinforcement. *Prog. Polym. Sci.*, 2008, **33**, P. 683–731.
- [14] Adachi K., Kotaka T. Dielectric normal mode relaxation. *Progr. Polym. Sci.*, 1993, **18**, P. 585–622.
- [15] Boyer R.F. Dependence of mechanical properties on molecular motion in polymers. *Polym. Eng. Sci.*, 1968, **8**, P. 161–185.
- [16] Liu H., Brinson L.C. Reinforcing efficiency of nanoparticles: a simple comparison for nanocomposites. *Compos. Sci. Tech.*, 2008, **68**, P. 1502–1512.
- [17] Rathmanathan K., Cavaille J.Y., Johari J.P. The dielectric properties of dry and water- Saturated nylon 12. *J. Polym. Sci. Part B. Polym. Phys.*, 1992, **30**, P. 341–348.
- [18] Laredo E., Hernandez M.C. Moisture effect on the low- and high-temperature dielectric relaxations in nylon-6. *J. Polym. Sci. Part B. Polym. Phys.*, 1997, **35**, P. 2879–2888.
- [19] Starkweather Jr.H.W., Avakian P. Conductivity and the electric modulus in polymers. *J. Polym. Sci. Part B. Polym. Phys.*, 1992, **30**, P. 637–641.
- [20] Havriliak S., Negami S., A complex plane analysis of α -dispersions in some polymer systems. *J. Polym. Sci. Part C*, 1966, **14**, P. 99–117.
- [21] Havriliak S., Negami S., A complex plane representation of dielectric and mechanical relaxation processes in some polymers. *Polymer*, 1967, **8**, P. 161–210.
- [22] Kremer F., Schonhals A. *Broadband dielectric spectroscopy*. Springer, New York, 2003.
- [23] Angell C.A., Ngai K.L., et al. Relaxation in glassforming liquids and amorphous solids. *J. Appl. Phys.*, 2000, **88**, 3113.
- [24] Plazek D.J., Magil J.H. Physical properties of aromatic hydrocarbons I. *J. Chem. Phys.*, 1998, **35**, P. 3038–3050.
- [25] Bureau E., Cabot C., Marais S., Saiter J.M. Study of the γ -relaxation of PVC, EVA and 50/50 EVA70/PVC blend. *Eur. Polym. J.*, 2005, **41**, P. 1152–1158.
- [26] Treacy M.M.J., Ebesen T.W., Gibson J.M. Nanoparticles as reinforced agents. *Nature (London)*, 1996, **381**, P. 678–680.
- [27] Schaefer D.W., Justice R.S. How nano are nanocomposites. *Macromolecules*, 2007, **40**, P. 8501–8517.
- [28] Sinitin A.N., Zuev V.V. Dielectric relaxation of fulleroid materials filled PA6 composites and the study of its mechanical performance. *Nanosystems: physics, chemistry, mathematics*, 2015, **6**, P. 570–582.
- [29] Baird M.E., Goldworthy G., Creasey C.J. Low frequency dielectric behavior of polyamides. *Polymer*, 1971, **12**, P. 159–175.